Available online at www.sciencedirect.com
ScienceDirect
Surface Science 601 (2007) 1554–1559
SURFACE SCIENCE
www.elsevier.com/locate/susc

Current–distance–voltage characteristics of electron tunneling through an electrochemical STM junction

D-H. Woo [a], E-M. Choi [a], Y-H. Yoon [a], K-J. Kim [a], I.C. Jeon [b], H. Kang [a,*]

[a] Department of Chemistry, Seoul National University, Gwanak-gu, Seoul 151-747, Republic of Korea
[b] Department of Chemistry, Jeonbuk National University, Jeonbuk 560-756, Republic of Korea

Received 4 December 2006; accepted for publication 16 January 2007
Available online 24 January 2007

Abstract

We have studied the electron tunneling process through an electrochemical scanning tunneling microscopic (STM) junction formed by a gold tip and a gold electrode immersed in an inert $NaClO_4$ solution. Current–distance–voltage characteristics of the tunneling process are examined by simultaneous measurement of tunneling current, voltage, and distance. The results indicate that the tunneling voltage across the junction changes with tunneling distance; however, tunneling conductance is an inverse exponential function of distance over the entire investigated range of tunneling current, voltage, and distance. The results provide clear evidence for the validity of a one-dimensional tunneling model for the aqueous tunneling process. Implications of the observation are mentioned with regard to the distance-dependent STM imaging and the origin of a low tunneling barrier height.

Keywords: Scanning tunneling microscopy (STM); Electrochemistry; Gold electrode; Electron tunneling; Tunneling barrier height

1. Introduction

The electrochemical STM has now become an important tool for the investigation of electrode surface structures, reactions, and electrochemical interfaces [1–4]. The fundamental mechanism of its operation in aqueous solution, in particular the electron tunneling process through the interfacial water layer, is however still not completely understood [5,6]. Electron tunneling through water is an important phenomenon related not only to the mechanism of electrochemical STM imaging, but also to various types of heterogeneous electron transfer processes occurring in aqueous environments such as electrode reaction, biological photosynthesis, and respiration.

The tunneling process in electrochemical STM experiments has been found to exhibit quite different characteristics from that in vacuum, according to the observations of previous studies [1–4,7–20]. Binggeli et al. [7] first studied the relationship between tunneling current and distance in an electrolyte solution, reporting that the tunneling distance is substantially longer (<10 Å for a tunneling resistance $<10^7\ \Omega$) in aqueous solution than that measured in vacuum (<3 Å). Ever since, the elongated tunneling distance has been confirmed by experiments performed under various electrochemical environments [8–20]. The tunneling barrier height measured in these experiments ranges between 0.1 and 2 eV, much lower than the values measured in vacuum, which are typically 3–5 eV [21].

The electrochemical STM results have generally been interpreted using a one-dimensional tunneling model. According to this model, the relationship between tunneling current (I_t), tunneling voltage (V_t), and gap distance (s) is expressed by Eq. (1), if the density of states of the metal surfaces is assumed to be structureless and the energy barrier is rectangular [21].

$$I_t \propto V_t \exp(-1.025\sqrt{\varphi}s) \tag{1}$$

Here φ is the tunneling barrier height given in eV, and s is in Å. Electrochemical STM experiments [7–18] have

* Corresponding author. Tel.: +82 2 8757471; fax: +82 2 889 1568.
E-mail address: surfion@snu.ac.kr (H. Kang).

0039-6028/$ - see front matter © 2007 Elsevier B.V. All rights reserved.
doi:10.1016/j.susc.2007.01.021

observed that the dependence of tunneling current on distance approximately follows Eq. (1). Some uncertainties in the early measurements of I_t–s behavior may be attributed to the fact that the tip-surface contact has not been precisely defined. In recent studies [18,19] the exponential I_t–s characteristics are observed for distances to the point of tip-surface contact, at which the tunneling resistance is close to the quantum resistance. Under certain conditions, however, the observed I_t–s curves deviate substantially from the exponential behavior [9,13–15]. The nonexponential I_t–s behavior suggests that the tunneling process involved in electrochemical STM imaging may be more complicated than that described by the one-dimensional tunneling model. Although, the model has been generally assumed to be applicable to the cases of electrochemical STM study, the validity of the model thus far has not been rigorously examined. Further, systematic investigation will be necessary on this issue.

For a thorough examination of the electrochemical tunneling process, it is required to control the tunneling parameters (I_t, V_t, and s) separately and measure them simultaneously during the STM experiment. It may not simply be assumed that these parameters are constant if they are not externally controlled, as will be demonstrated in this work. In the present study, we prepare an STM junction in electrochemically well-defined conditions by gold electrodes and an inert electrolyte solution. The I_t–V_t–s characteristics of the tunneling process are examined through simultaneous measurements of I_t, V_t, and s, based on which the validity of a one-dimensional tunneling model is discussed.

2. Experimental methods

The electrochemical STM used for the experiment is schematically shown in Fig. 1. The electrochemical cell consisted of working (WE), reference (RE), and counter electrodes (CE), and a tip, all made of gold, immersed in an aqueous solution of $NaClO_4$ or in pure water. The tip and the WE formed a tunneling junction filled with solution. The WE was a gold film deposited on a glass substrate, cleaned in a piranha solution and annealed by a hydrogen flame. A gold film thus prepared showed wide terraces of a (1 1 1) crystalline face in an STM image and the cyclic voltammetric (CV) features characteristic of an Au(1 1 1) electrode surface in $NaClO_4$ and $HClO_4$ solutions [22]. The tip was fabricated by electrochemical etching of a gold wire and coating with a nitrocellulose varnish material except at its apex [23]. The exposed gold apex, with an area smaller than 10 μm^2 as estimated from the limiting currents of CV for the $Fe(CN)_6^{3-}/Fe(CN)_6^{4-}$ redox reaction, produced negligibly small faradic currents (<30 pA) during the STM experiment. The electrode potentials and the tunneling bias voltage (V_b) were set by a bipotentiostat (Pine model AFRDE5). The potentials of WE and the tip were varied within the double-layer region (0–600 mV against the Ag/AgCl electrode), in which the specific adsorption

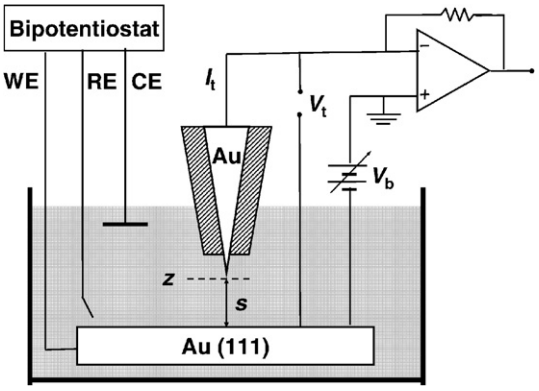

Fig. 1. Schematic diagram of the electrochemical STM setup. A bipotentiostat controls the electrode potentials and the tunneling bias voltage V_b. As we move a gold tip slowly toward a gold WE surface, we simultaneously measure I_t by a current amplifier and V_t by a high input-impedance potentiometer (not shown). The labels z and s denote the tip apex position and the gap distance, respectively, along the normal direction to the WE surface.

of ClO_4^- is known not to occur on a gold surface [24]. The solution was prepared with deionized water having a specific resistivity of 18 MΩ cm, and was bubbled with N_2 gas before use to remove the dissolved oxygen species.

In the tip-approach experiment, we drove an STM tip from an initial tunneling position toward the surface of WE by a piezo driver with the tunneling current feedback-loop disabled. The tunneling current was measured by a current amplifier as a function of the tip-approach distance. The actual voltage across a tunneling gap (V_t) was simultaneously measured along the tip-approach by a potentiometer with a high input impedance ($\geqslant 1 \times 10^{12}$ Ω). In the voltage-scan experiment, we externally changed the tunneling bias voltage (V_b), while keeping the tunneling current at a constant value by the current feedback. The displacement (Δz) of a tip-resulting from the V_b change was measured from the known sensitivity of a piezo driver. The rates of tip-approach and voltage scan were controlled so that the thermal drift (<1 Å s^{-1}) in gap distance did not significantly affect the measurement.

3. Results and discussion

3.1. Current–distance relationship

Fig. 2 shows the result of the tip-approach experiment obtained in an $NaClO_4$ solution of 1 mM concentration. V_b is fixed at −100 mV, where the bias voltage is applied at a WE against the ground potential of a tip. The I_t–s curve shows that the tunneling current increases exponentially with decrease in the gap distance, only when the tip and the WE surface are far apart. At small distances the I_t–s curve does not follow an exponential behavior. Fig. 2 also shows the measurement of the actual tunneling voltage (V_t) during the approach experiment, made by connecting a voltage preamplifier with a high input impedance ($\geqslant 1 \times$

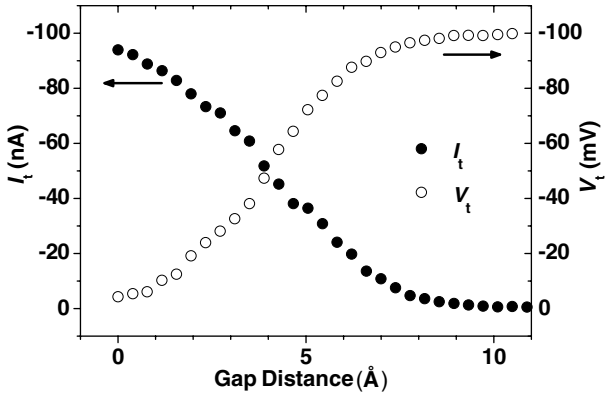

Fig. 2. Variation in tunneling current (I_t) and tunneling voltage (V_t) as a function of gap distance (s). The tip was initially located at an equilibrium distance corresponding to $I_t = 0.3$ nA in a 1 mM $NaClO_4$ solution, and was moved toward the WE surface ($s = 0$ Å) at an approach speed of 50 Å s^{-1}. V_b was −100 mV. The WE potential was 16 mV against a gold RE.

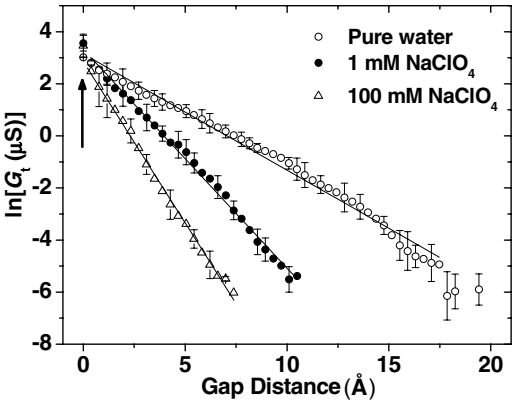

Fig. 3. Tunneling conductance measured as a function of gap distance in pure water and $NaClO_4$ solutions. The arrow indicates the bending of conductance curves due to a tip-surface contact. The results shown are the average of several repeated measurements on a single system, with the data fluctuations represented by the error bars. $V_b = -100$ mV in $NaClO_4$ results and $V_b = 100$ mV in pure water. The tip approach speed is 50 Å s^{-1}.

10^{12} Ω) directly across the tunneling gap. The V_t–s curve reveals that V_t is close to the externally applied tunneling voltage (V_b) at a long tunneling distance, but V_t decreases for $s < 8$ Å. This behavior can be attributed to a decrease in the tunneling resistance at close proximity to a substrate surface; V_b is divided between the reduced tunneling resistance and the input impedance of the current preamplifier. The effect of reduced V_t on the I_t–s measurement was first reported by an STM study in vacuum [25]. As shown in Fig. 2, this effect starts to occur at a substantially longer distance (<8 Å) in the electrochemical environment than in vacuum (<2 Å). The measured V_t–s curve can be closely traced by accounting for the voltage drop across a fixed input resistance of a current amplifier circuit, $V_t = V_b - I_t R_{input}$, from which R_{input} is estimated to be 1.04×10^6 Ω for the present instrument by curve fitting.

Tunneling conductance, $G_t = I_t/V_t$, is calculated from the result of simultaneous measurements of I_t and V_t. Fig. 3 shows the $\ln G_t$ vs. s plots for the results obtained in pure water and $NaClO_4$ solutions of 1 mM and 100 mM concentration. The plots show good linearity in the investigated ranges of tunneling distance. This observation is in conformity with the G_t–s relationship in the one-dimensional tunneling model (Eq. (2)).

$$G_t = I_t/V_t = G_0 \exp(-1.025\sqrt{\varphi}s) \quad (2)$$

where G_0 is the conductance at $s = 0$ Å. The data measured in pure water fall slightly below the line at long distances (>15 Å), but the degree of deviation from linearity is within the experimental uncertainty and does not represent a general feature. It is reported [18,19] that the $\ln G_t$–s plot is modulated with weak periodic oscillations coinciding with the structure of interfacial water layer. In the present study, such extra features disappear after averaging the results of repeated tip-approach experiments. Whereas, the $\ln G_t$–s plots are linear, the corresponding $\ln I_t$–s plots (not shown) are obviously curved due to the drop in V_t at decreased tunneling distances. This indicates importance to measure $G_t = I_t/V_t$, not I_t alone, in the electrochemical STM experiment, because the V_t drop can be significant even at a relatively long distance.

The linear $\ln G_t$–s plot bends sharply upward upon electrical contact of the tip, and the electrode surface [26], as indicated by the arrow in Fig. 3. This position defines the zero gap distance. The conductance value at the contact position is measured to be $G_0 = 20 \pm 4$ μS (1 siemens = 1 Ω^{-1}) in the three plots. This value agrees with 8–20 μS measured between Au tips and Au(1 1 1) surfaces in electrolyte solutions [18,19] and 20–40 μS between metal tips and Au(1 1 0) surfaces in vacuum [25], thereby supporting the assignment of the contact position.

The apparent tunneling barrier height, φ, can be deduced from the slope of a $\ln G_t$–s plot. Since the $\ln G_t$–s plots are linear over the examined range of tunneling distance, it can be said that φ is constant in this range. If a curved $\ln I_t$–s plot was used to deduce φ, an erroneous behavior of φ changing with s would appear. In Fig. 3, φ is deduced to be 0.17 eV in pure water, 0.62 eV in a 1 mM solution, and 1.6 eV in a 100 mM solution. These φ values fall into the range of values in the literature [8–20]. We have observed that the measured φ values do not show a systematic dependence on electrolyte concentration, though such a trend might seem to exist in the particular data set of Fig. 3. The measurements at different bias voltages also produce randomly distributed φ values.

3.2. Distance–voltage relationship

We examined the relationship between tunneling voltage and distance. The explicit form of the voltage–distance relationship in a one-dimensional model is given by Eq. (3), which is a rearranged form of Eq. (1)

$$\ln I_t = \ln V_t - 1.025\sqrt{\varphi}s + \alpha \quad (3)$$

where α is a constant. Eq. (3) predicts a linear dependence between s and $\ln V_t$ for a fixed value of I_t. In the s–$\ln V_t$ measurement, we scanned V_b, while keeping I_t at a constant value through the current feedback, and the resulting change in tip position (Δz) was recorded. The Δz–V_b measurement of STM has not been reported to the best of our knowledge. Fig. 4 shows the result obtained with V_b ramping between -10 mV and -290 mV in forward and backward directions at $I_t = 0.3$ nA in a $NaClO_4$ solution of 1 mM concentration. During the V_b scan, the potential of WE (E_{WE}) with respect to RE was kept constant in order not to change the electrical double layer (EDL) property at the WE. This was done by changing the RE potential (the inner potential of the solution) with respect to the ground by the same amount as a V_b change using a bipotentiostat. The electrode potentials applied are described in the figure caption. The Δz–V_b curves in Fig. 4 exhibit a semi-logarithmic behavior. As the magnitude of tunneling voltage is increased from $|V_b| = 10$ mV to 290 mV, the tunneling distance increases by about 8 Å.

To test the semi-logarithmic dependence of Δz on V_b appearing in Fig. 4, we plot Δz against $\ln V_b$. Further, the Δz measurement is converted into a scale of absolute tunneling distance. This is done by calculating the tunneling distance for given values of I_t and V_t, using the linear $\ln G_t$–s relationship and the reference value of $G_t = 20$ μS at $s = 0$ Å. Fig. 5 shows the s-$\ln V_t$ plots obtained by this procedure for a series of Δz–V_b measurements made in water and $NaClO_4$ solutions with different concentrations. The tunneling voltage is scanned between $|V_b| = 3$–30 mV (corresponding to $|V_t| = 2.5$–30 mV) at a rate of 10 mV s^{-1} for $I_t = 0.3$ nA. Another data set for pure water is included in the figure to exemplify the result of a wide range scan ($|V_b| = 5$–200 mV) made at a faster rate (100 mV s^{-1}) with a different tip. All these plots appear linear, confirming the semi-logarithmic dependence of s on V_t. The linearity holds basically for the entire range of investigation, which

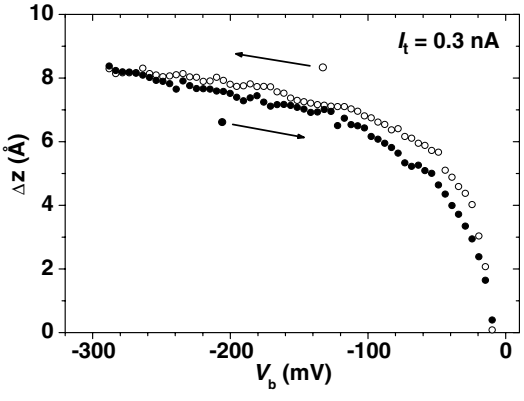

Fig. 4. Δz–V_b curves for V_b scans between -10 mV and -290 mV at $I_t = 0.3$ nA in 1 mM $NaClO_4$ solution. The arrows indicate the direction of V_b ramping. Increasing Δz is away from the surface. The data shown are the average of four scans. During the V_b ramping, E_{WE} was maintained constant at -50 mV, by simultaneously ramping the RE potential with respect to the ground between 40 mV and -240 mV.

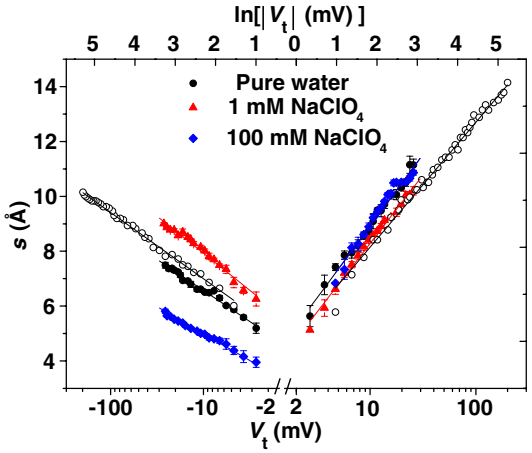

Fig. 5. Tunneling distance vs. voltage measured at $I_t = 0.3$ nA in pure water and $NaClO_4$ solutions. The plots for $|V_t| = 2.5$–30 mV are the averages of four repeated scans, and the plots for $|V_t| = 5$–200 mV are single scan results.

encompasses $|V_t| = 2.5$–200 mV, and the corresponding tunneling distance of 4–12 Å.

The inverse of the slope of the s–$\ln V_t$ plot gives the tunneling barrier height. The φ values deduced from the narrow scan data in Fig. 5 for positive (negative) bias polarity are 0.56 eV (1.04 eV) in pure water, 0.66 eV (0.73 eV) in 1 mM solution, and 0.60 eV (1.76 eV) in 100 mM solution. The result of φ measurements varies greatly for different Au tips, even when all the other experimental conditions are prepared to be the same. Such behavior is observed for both Δz–V_b and I_t–s measurements. In Fig. 5, for example, the two plots obtained in pure water by the narrow and wide scans of V_b do not overlap well, as they are measured with different tips. Each plot, however, is linear by itself and self-consistent.

In another experiment, we changed the WE potential (E_{WE}), while keeping both V_b and I_t constant, in order to examine the effect of the electrochemical environment of WE on the tunneling process. E_{WE} was scanned between -300 and 300 mV against a gold RE (0–600 mV against an Ag/AgCl electrode). The potential change in this "double-layer region" would not cause additional electrochemical reaction at the WE in $NaClO_4$ solution [24], and only the EDL structure at WE would change. The result shows that the change in E_{WE} by 600 mV changes the tunneling distance by 1.8 Å. Thus, E_{WE} affects the tunneling distance but only weakly compared to V_b. The tunneling distance linearly increases with increase in E_{WE} toward a more positive value, when a negative tunneling voltage is applied at WE. The observed weak dependence of tunneling on E_{WE} is consistent with the results obtained with a Pt/Ir tip and a gold WE in $NaClO_4$ solution [8].

3.3. Tunneling barrier height

The barrier height measurement from the $\ln G_t$–s (Fig. 3) and s–$\ln V_t$ plots (Fig. 5) shows φ values ranging between

0.23 and 1.8 eV, which are in general agreement with the previously reported values [8–20]. The result of the φ measurement, however, varies greatly and randomly depending on the tips used, as mentioned above. This hampers systematic investigation for the effects on φ of electrochemical parameters such as electrolyte concentration, WE potential, and the polarity of the tunneling voltage. Nevertheless, at least one aspect of the φ measurement is noteworthy. Despite, the variation of φ with the tips and electrochemical conditions, φ is invariant with respect to the changes in s, I_t, and V_t in each experiment performed with an individual tip, as is evident in the linear plots of $\ln G_t$–s and s–$\ln V_t$. This observation is logically consistent with the one-dimensional tunneling model, in which φ is independent from s, I_t, and V_t; there is no a priori reason to expect interdependency between φ and these variables.

We may discuss the possible origin of the low barrier height, a longstanding issue in electrochemical STM study, in relation to the present observations. It has been suggested [20] that the experimental φ value may be lowered due to elastic deformation of an STM junction caused by the tip-pressure, which changes the actual gap distance and, in turn, the slope of the modified conductance–distance plot. The linear proportionality between $\ln G_t$ and the tip displacement (Δz) over a wide range of distances to the tip-surface contact, which result is in quantitative agreement with Eq. (2), indicates that the $\Delta z/\Delta s$ ratio is constant and equal to unity during the experiment. Thus, there must not be significant deformation of the STM junction caused by the tip-pressure. The linear $\ln G_t$–s behavior also denies the possible presence of Ohmic leakage currents, including those flowing through the impurity molecules bridging an STM gap, which intervene with the tunneling current measurement; the leakage currents would exhibit a different distance-dependence from that of the tunneling current. It is difficult to completely remove the impurity species from the electrochemical cell used for the STM study. For this reason, it is suggested that the impurities in solution or adsorbed on electrode surfaces may provide intermediate tunneling states that lead to the lowering of φ [10]. In the shortest limit of tunneling distance investigated in the present study, however, there seems not to be enough space between the tip and the surface to accommodate the impurity molecules. The linear $\ln G_t$–s and s–$\ln V_t$ plots nevertheless extend to such impurity-free distances and also to the point of tip-surface contact. This implies that the tunneling process is not governed by the impurity species.

The effect of EDL on the tunneling process may also be considered. The observation shows that the tunneling distance and φ are only weakly affected by the WE potential which affects the EDL. Also, φ stays rather constant as the tip penetrates into the EDL at WE. These observations suggest only minor influence of EDL on the tunneling process. Since a tunneling distance is usually shorter than the Debye length of an EDL, the EDLs at the tip and WE surfaces will show significant overlap during electrochemical STM experiments to modify the EDLs [27,28]. If this happens, it will be difficult to properly assess the effect of EDL on the tunneling process. To summarize the discussions above, the impurity and tip-pressure effects on φ can be excluded, and the several different possibilities may be narrowed down to the interpretation that the lowering of φ reflects the inherent nature of the electron tunneling process through an electrochemical STM junction.

4. Conclusion

We have examined the I_t–V_t–s characteristics of an STM junction made of a gold tip and a gold electrode immersed in an inert electrolyte solution by simultaneous measurement of I_t, V_t, and s. The observed linear $\ln G_t$–s and s–$\ln V_t$ relationships reveal that the one-dimensional tunneling model of Eq. (2) is valid for the aqueous tunneling process over a wide range of distance and for V_t smaller than the tunneling barrier height. This conclusion has thus far been assumed in electrochemical STM works without full experimental support. The study also points out that V_t can significantly change at a short tip-surface distance, a condition that is often employed in electrochemical STM experiment to resolve the images of electrode surface and adsorbate layers. The distance-dependent STM images obtained under such low-conductance conditions therefore may need to be interpreted by accounting for the associated V_t change. Finally, the observation of a constant tunneling-barrier height for the changes in I_t, V_t, and s suggests that the low barrier height measured in an aqueous environment may represent an intrinsic property of the tunneling process through a metal/water/metal junction.

Acknowledgement

This work was supported by the Nano Systems Institute through a National Core Research Center program and by the Korea Research Foundation.

References

[1] K. Itaya, Prog. Surf. Sci. 58 (1998) 121.
[2] N.J. Tao, C.Z. Li, H.X. He, J. Electroanal. Chem. 492 (2000) 81.
[3] D.M. Kolb, Surf. Sci. 500 (2002) 722.
[4] D. Friebel, C. Schlaup, P. Broekmann, K. Wandelt, Surf. Sci. 600 (2006) 2800.
[5] W. Schmickler, Surf. Sci. 335 (1995) 416.
[6] A. Nitzan, I. Benjamin, Acc. Chem. Res. 32 (1999) 854.
[7] M. Binggeli, D. Carnal, R. Nyffenegger, H. Siegenthaler, R. Christoph, H. Rohrer, J. Vac. Sci. Technol. B 9 (1991) 1985.
[8] J. Pan, T.W. Jing, S.M. Lindsay, J. Phys. Chem. 98 (1994) 4205.
[9] A. Vaught, T.W. Jing, S.M. Lindsay, Chem. Phys. Lett. 236 (1995) 306.
[10] J. Halbritter, G. Repphun, S. Vinzelberg, G. Staikov, W.J. Lorenz, Electrochim. Acta 40 (1995) 1385.
[11] C. Kobusch, J.W. Schultze, Electrochim. Acta 40 (1995) 1395.
[12] Y. Nagatani, T. Hayashi, T. Yamada, K. Itaya, Jpn. J. Appl. Phys. 35 (1996) 720.
[13] G. Nagy, G. Denault, J. Electroanal. Chem. 437 (1997) 37.

[14] G. Nagy, T. Wandlowski, Langmuir 19 (2003) 10271.
[15] G.E. Engelmann, J.C. Ziegler, D.M. Kolb, Surf. Sci. 401 (1998) L420.
[16] J. Ahn, M. Pyo, Bull. Kor. Chem. Soc. 21 (2000) 644.
[17] M.B. Song, J.M. Jang, S.E. Bae, C.W. Lee, Langmuir 18 (2002) 2780.
[18] P. Hugelmann, W. Schindler, Surf. Sci. 541 (2003) L643.
[19] P. Hugelmann, W. Schindler, J. Phys. Chem. B 109 (2005) 6262.
[20] S.C. Meepagala, F. Real, Phys. Rev. B. 49 (1994) 10761.
[21] R. Wiesendanger, Scanning Probe Microscopy and Spectroscopy, Cambridge University Press, 1994.
[22] R.P. Janek, W.R. Fawcett, A. Ulman, J. Phys. Chem. B 101 (1997) 8550.
[23] D-H. Woo, H. Kang, S-M. Park, Anal. Chem. 75 (2003) 6732.
[24] A. Hamelin, T. Vitanov, E. Sevastyanov, A. Popov, J. Electroanal.Chem. 145 (1983) 225.
[25] L. Olesen, M. Branbyge, M.R. Sorensen, K.W. Jacobsen, E. Lægsgaard, I. Stensgaard, F. Besenbacher, Phys. Rev. Lett. 76 (1996) 1485.
[26] The apparent tunneling barrier height decreases with decreasing gap distance according to theoretical calculations obtained with a static model of STM junction in vacuum N.D. Lang, Phys. Rev. B 36 (1987) 8173;
N.D. Lang, Phys. Rev. B 37 (1988) 10395, When the atomic relaxation of the junction is taken into account, it is shown [25] that the barrier height stays nearly constant all the way to point contact.
[27] E.J.W. Verwey, J.Th.G. Overbeek, Theory of the Stability of Lyophoic Colloids, Elsevier, Amsterdam, 1948.
[28] D-H. Woo, J-S. Yoo, S-M. Park, I.C. Jeon, H. Kang, Bull. Kor. Chem. Soc. 25 (2004) 577.